Published in final edited form as:
Biochemistry. 2009 February 17; 48(6): 1390–1398. doi:10.1021/bi801901d.

Association Energetics of Cross-reactive and Specific Antibodies

S. Mohan[1,3], **Katerina Kourentzi**[1], **Kari A. Schick**[1,4], **Christian Uehara**[1], **Claudia A. Lipschultz**[5], **Mauro Acchione**[5], **Morgan E. DeSantis**[5], **Sandra J. Smith-Gill**[5], and **Richard C. Willson**[1,2,*]

[1]Department of Chemical & Biomolecular Engineering, University of Houston, Houston, TX 77204-4004

[2]Department of Biology and Biochemistry, University of Houston, Houston, TX 77204-5001

[5]Structural Biophysics Laboratory, Center for Cancer Research, National Cancer Institute, Frederick, MD 21702-1201

Abstract

HyHEL-8, HyHEL-10 and HyHEL-26 (HH8, HH10 and HH26, respectively) are murine monoclonal IgG_1 antibodies which share over 90% variable-region amino acid sequence identity and recognize identical structurally-characterized epitopes on hen egg white lysozyme (HEL). Previous immunochemical and surface plasmon resonance-based studies have shown that these antibodies differ widely in their tolerance of mutations in the epitope. While HH8 is the most cross-reactive, HH26 is rigidified by a more-extensive network of intramolecular salt links, and is highly specific, with both association and dissociation rates strongly affected by epitope mutations. HH10 is of intermediate specificity, and epitope mutations produce changes primarily in the dissociation rate. Calorimetric characterization of the association energetics of these three antibodies with the native antigen HEL and with Japanese quail egg white lysozyme (JQL), a naturally occurring avian variant, shows that the energetics of interaction correlate with cross-reactivity and specificity. These results suggest that the greater cross-reactivity of HH8 may be mediated by a combination of conformational flexibility and less specific intermolecular interactions. Thermodynamic calculations suggest that upon association HH8 incurs the largest configurational entropic penalty and also the smallest loss of enthalpic driving force with variant antigen. Much smaller structural perturbations are expected in the formation of the less flexible HH26 complex, and the large loss of enthalpic driving force observed with variant antigen reflects its specificity. The observed thermodynamic parameters correlate well with the observed functional behavior of the antibodies and illustrate fundamental differences in thermodynamic characteristics between cross-reactive and specific molecular recognition.

Keywords

Protein-protein recognition; antibody-antigen complexes; cross-reactivity and specificity; titration calorimetry; affinity maturation; thermodynamics

The association of antibodies with antigens is a critical component of immune function, and the processes of recognition and association are underlying features of all protein-protein interactions. The immune system is, however, unique in the occurrence of both highly specific and non-specific (cross-reactive and poly-reactive) interactions involving different types of

*Corresponding author: E-mail: Willson@uh.edu, Phone: (713) 743-4308, Fax: (713) 743-4323.
[3]Present address: Medarex, Inc., 1324 Chesapeake Terrace, Sunnyvale, CA 94089
[4]Pesent address: 7413 Churchill Square, Mentor, OH 44060

antibodies. An understanding of antibody-antigen association is of growing importance for engineering of antibodies for therapeutic and diagnostic applications. Several antibody-antigen complexes have been extensively characterized not only for their immunological and clinical interest, but also as model systems to elucidate the general principles of protein-protein interactions (1–3). Antibodies recognizing hen egg white lysozyme (HEL) have often been used, with the majority of these studies addressing molecular, thermodynamic and kinetic features of antibodies with high specificity. There are significantly fewer reports addressing the molecular basis of recognition by cross- and poly-reactive or heteroclitic antibodies.

In this work we demonstrate for the first time that the associations of cross-reactive and specific antibodies differ thermodynamically in a systematic way. HyHEL-8 (HH8) and HyHEL-26 (HH26) are high-affinity anti-HEL antibodies which recognize the same structurally characterized epitope as the HyHEL-10 (HH10) antibody (4–8). While HH26 is highly specific, HH8 is significantly more cross-reactive and tolerant of epitope mutations that significantly inhibit or abolish the binding of HH26. The degree of specificity or cross-reactivity of HH10 lies between that of HH8 and HH26. Previous reports on this family of antibodies by Smith-Gill *et al.* (4,5,9–12) have led to an understanding of some of the molecular origins of their functional differences, especially in their kinetics of association and dissociation.

Here we present a thermodynamic comparison of HH10 complex formation with HEL and the natural epitope variant Japanese quail egg white lysozyme (JQL) containing the hotspot mutation R21Q, as well as three other mutations in the epitope, with the corresponding complexes of HH8 and HH26 using isothermal titration calorimetry. The results obtained advance our understanding of the specificity of antibodies and their cross-reactivity with mutant antigens.

Materials and Methods

Antibody Production and Purification

Supernatant enriched with HH10 IgG was produced at the National Cancer Institute as previously described (7). The supernatants of hybridoma cell lines producing the HH8 and HH26 monoclonal antibodies (7,13,14) were produced by the National Cell Culture Center and stored at −80°C until purification.

HH10 protein was purified by sequential anion-exchange, hydroxyapatite and hydrophobic interaction chromatography. Anion exchange chromatography used a Q Sepharose Fast Flow column (diameter: 2.5 cm; length: 25 cm) (GE Healthcare). The column was equilibrated with 50 mM Tris, 0.1 mM EDTA, pH 8.0 (buffer A). After loading, the column was washed with buffer A and protein was eluted with a gradient of NaCl in buffer A (0 −400 mM; 25 column volumes). Peaks containing the antibody were identified by silver-stained 8–25% gradient SDS-PAGE gels (PhastSystem; GE Healthcare) or dot blot immunoassays, then pooled and dialyzed in 10 mM sodium phosphate, pH 6.8 in preparation for the hydroxyapatite column. The dot blot immunoassays were based on the binding of HH10 (pre-incubated for two hours with and without 1 mg/ml HEL) to HEL adsorbed on nitrocellulose membranes (Pierce). This HEL competition assay was used to distinguish between specific and nonspecific adsorption. Membranes were blocked with 3% nonfat dry milk before binding the HH10 samples, and HH10 was detected with a protein G-alkaline phosphatase conjugate (Pierce) using the BCIP/NBT (Pierce) chromogenic substrate as described by the manufacturer.

The pooled ion-exchange fractions were further purified by hydroxyapatite chromatography (Bio-Gel HT; BioRad; diameter: 2.5 cm; length: 60 cm). The HH10 antibody was eluted using a gradient of sodium phosphate, pH 6.8, (10 −300 mM; 5 column volumes). Fractions containing HH10 were pooled and concentrated to a final volume of *ca.* 20 ml using a stirred

ultrafiltration cell with a YM10 membrane (Spectrum, Gardena, CA) and then dialyzed overnight in 10 mM Tris, 1 M NaCl, pH 7.0 in preparation for hydrophobic interaction chromatography.

The hydrophobic interaction adsorbent used was Phenyl Sepharose (GE Healthcare; column diameter: 2.5 cm; length: 25 cm). The isocratic eluant (10 mM Tris + 1 M NaCl, pH 7.0) was chosen to prevent HH10 adsorption, while promoting BSA adsorption (the primary contaminant remaining after the hydroxyapatite chromatography step). Fractions containing HH10 were concentrated to ≥1 mg/ml using a stirred ultrafiltration cell (Spectrum, Gardena, CA). SDS-PAGE was used to assess purity of the final HH10 antibody preparation and showed only bands corresponding to the antibody heavy and light chains. The binding activity of the final HH10 preparation was assayed by dot-blot as described previously (15).

HH8 and HH26 were purified using the Protein A or Protein A/G columns from the ImmunoPure IgG purification kit (Pierce). Purified proteins were checked for purity on silver-stained Phast SDS-PAGE gels (GE Healthcare).

Lysozyme Purification

HEL (2x crystallized) was obtained from Worthington (Freehold, NJ). Size exclusion chromatography and silver-stained SDS-PAGE were used to establish that the HEL used (lot number 32C875) was at least 99% pure and free of aggregates. HEL activity was also tested using the *Micrococcus lysodeikticus* lysis assay (16).

Japanese quail eggs were obtained from Stevenson Game Bird Farm (Riverside, TX) and from Truslow Farms, Inc. (Chestertown, MD); Truslow Farms was a supplier used in the earlier study of Lavoie *et al.* (4). JQL from both sources exhibited identical calorimetric results, and the results reported are those obtained using the eggs from Stevenson Game Bird Farm. Upon receipt the egg white was separated from the yolk and stored at −80°C for later purification of lysozyme. The egg white was thawed and homogenized briefly in a Waring blender. This material was filtered through two layers of cheesecloth and then two layers of Kimwipes, diluted with six times the original egg white volume of 15 mM ammonium acetate, pH 9.2, and contacted with 10 g CM Sephadex (GE Healthcare) per 100 ml egg white at 4°C with gentle stirring. After overnight adsorption the supernatant was decanted and replaced with an equal volume of 15 mM ammonium acetate, pH 9.2 every hour until the liquid was clear (typically three times). The adsorbent was then packed into an empty 5 cm diameter chromatography column and the adsorbed proteins (largely JQL) were eluted with 500 mM ammonium acetate, pH 9.4. This material was concentrated using an ultrafiltration cell with a YM10 membrane (Spectrum, Gardena, CA) and loaded onto a Sephacryl S-100 HR (GE Healthcare) column (diameter: 2.5 cm; length: 40 cm). Loading volume was *ca.* 10 ml and the running buffer was 15 mM ammonium acetate, pH 9.2. During the purification the *Micrococcus lysodeikticus* lysis assay (16) was used to identify fractions containing lysozyme. Final purification was achieved using a CM Sepharose (GE Healthcare) column (diameter: 5 cm; length: 8 cm); lysozyme was eluted with a 1.0 L gradient of ammonium acetate, pH 9.2 (15 mM −500 mM). Lysozyme was the main peak eluting during the second half of the gradient and found to give a single band upon silver-stained SDS-PAGE analysis.

Sample Preparation for Calorimetry

Experiments were carried out in 10 mM sodium phosphate adjusted to pH 8.0 (except where noted) at the intended experimental temperature in an environmental room (NorLake Scientific, Hudson, WI). HH10 and HEL samples of *ca.* 5 ml each were co-dialyzed overnight at 4 °C against the same 4 L volume of buffer to ensure precise matching of the buffer concentration and pH. After dialysis, the concentrations of HEL and HH10 solutions were determined by

absorption measurements at 280 nm using a Beckman DU-64 spectrophotometer. The extinction coefficient used for HEL was $E_{281.5}$ = 2.64 (17), and the molecular mass used for HEL was 14,388 Da (18). The HEL extinction coefficient was also used for JQL since the two lysozymes differ in only one absorbance-active residue (Phe 3 to Tyr), which would produce a difference in the molar extinction coefficient of less than four percent (19). The molecular mass of HH10 was taken as 150,000 Da, and the extinction coefficient was estimated as E_{280} = 1.43 (K.A. Xavier, unpublished results) by the method of Gill and von Hippel (19) using the known HH10 Fv sequence and the constant region sequences of the murine (Balb/c) plasmacytoma MOPC-21 (20). HEL concentration was adjusted by the addition of dialysis buffer to a concentration that (after centrifugation as described below) would saturate all antibody binding sites near the midpoint of the calorimetric titration. All samples were centrifuged at 100,000 x*g* in a Beckman TL-100 ultracentrifuge for 30 minutes immediately before use. After centrifugation the final concentrations of antibody and lysozyme samples were determined spectrophotometrically. The A_{280} of protein samples was reduced by up to 25% after centrifugation, and they were free of any detectable scattering at wavelengths above 350 nm.

Isothermal Titration Calorimetry

An OMEGA isothermal titration calorimeter (Microcal, Northampton, MA) was used for all experiments as described previously (15,21). The design and operation of the instrument have been previously described by Wiseman, *et al.* (22). A voltage conditioner (Tripp Lite) and a ferroresonant transformer (General Signal) were connected in series for power stabilization, and a circulating water bath (Haake model A81) was used to stabilize the experimental temperature.

Data analysis was carried out as described previously (15,21) using ORIGIN, the data analysis software provided with the calorimeter. Manual peak-by-peak integration yielded better representations of the data than did the automatic baseline determination provided by the software. The integrated areas for injections prior to saturation typically varied by less than four percent and were averaged to obtain the apparent binding enthalpy. To obtain the reported enthalpies, the apparent binding enthalpy values were corrected for the small dilution enthalpy resulting from titrating HEL into HH10/HEL complex solution. This was determined by averaging the integrated areas obtained for injections after saturation. All calorimetric titrations were repeated at least twice.

SPR measurements

Pre-equilibrium rate constants for binding were determined using a Biacore 2000 (GE Healthcare Bio-Sciences, Uppsala, Sweden) instrument. Fabs refolded from *E. coli*inclusion bodies (6,9), were always used in order to study monovalent inherent affinities. Fab samples in HBS buffer (10 mM HEPES, 150 mM NaCl, 0.005% P20, pH 7.4) were injected over a CM5-dextran chip immobilized with different levels of amine-coupled HEL to provide surfaces that ranged from 60 response units (RUs) to 150 RUs. Previous SPR and fluorescence anisotropy studies have demonstrated that the interaction of these antibodies with HEL results in complex time dependant two-step binding kinetics (Equation 1) that are best evaluated using a series of different injection times (10,23).

$$A+B \underset{k_{-1}}{\overset{k_1}{\rightleftarrows}} AB^* \underset{k_{-2}}{\overset{k_2}{\rightleftarrows}} \mathrm{AB} \tag{1}$$

The SPR experimental protocol consisted of four analyte-inject (association) times of 10, 25, 60 and 120 min, followed by a two-hour dissociation phase with HBS buffer. Sensorgrams

were corrected using a blank flow cell from the same chip that had been exposed to the same amine-coupling protocol without protein. These corrected sensorgrams were then pooled for global analysis using the two-step model in the BiaEvaluation 3.0 (Equation 1). Representative SPR data and associated fits are given in the Supporting Information. $\Delta G°$ was calculated from the net binding affinity, K_A. Experiments with HH10 were performed at 10°C, 25°C, and 37°C. Calculations using SPR measurements of ΔG and ITC estimates of $\Delta H$and ΔC_p, with their experimental errors propagated for all calculations, showed that small differences among temperatures did not produce significant differences among the calculated entropy values. Reliable estimates of some rate constants at the highest and lowest temperatures are extremely difficult to obtain for HH26 and HH8 associations. This is because at 37°C very little HH26 binds to the surface, especially to JQL, k_{-1} is very high and k_2 is very low, making estimates unreliable. Similarly, at low temperatures, such as 10°C, rates are very slow, and in the case of HH8 observed off rates may be as low as only 1 or 2 RU during a 4-hour dissociation period. Even in the case of HH10 binding to JQL, some rate constants were difficult to measure, thus accounting for relatively high error rates in the ΔGestimates for these complexes. The empirically determined values of ΔGat all 3 temperatures were used for HH10 complexes (the variation with temperature is very small; see Table 2). To estimate ΔG values for HH26 and HH8 complexes at 10 and 37°C the non-linear van't Hoff equation (2) was used, using experimentally measured ΔG_0 at 25°C and experimental values of ΔC_p from ITC:

$$\Delta G_T = \Delta G_0 + \Delta C_p(T - T_0) - T \times \Delta C_p \times \ln\left(\frac{T}{T_0}\right) \quad (2)$$

where T_0 is the standard temperature, 25°C. This approach is supported by the observation that estimating ΔG_T values for HH10 at 10 and 37°C by the same method gave values that all were within the standard error of the observed 10 and 37°C data (data not shown).

Results

Association energetics of HH10 with HEL and JQL

Figure 1 shows the results of the calorimetric titration of HH8 with HEL; these results are representative of the high-affinity HEL titration of all three antibodies. The top panel shows the raw titration data and the bottom panel shows the integrated area for each injection, as a function of the molar ratio of HEL to total antibody binding sites. The high affinity of antibody/HEL association precludes the determination of affinity by calorimetric titration, as described by Wiseman *et al.* (22). Experiments were designed, therefore, to facilitate accurate measurement of the enthalpy and stoichiometry of antibody/HEL binding, and the small apparent HEL heat of dilution. Dilution-corrected heats of association for HH10/HEL association are shown in Table 1, along with the standard deviation associated with each value of ΔH.

Table 1 also presents the experimental equivalence ratio (typically 0.80), determined by dividing the number of moles of lysozyme present in the cell at the calorimetrically indicated stoichiometric equivalence by the number of moles of antibody combining sites present (15, 21). Deviation from unity can be attributed to the presence of inactive antibody molecules or impurities and/or inaccuracies in the antibody molecular mass or extinction coefficient used. Injection of lysozyme, for which the mass and extinction coefficients are better known, increases the precision of the energetic measurements. Table 1 lists values of HH10/HEL association enthalpies in 10 mM sodium phosphate, pH 8.0 at temperatures ranging from 10°C to 37°C. As a control for proton liberation or uptake upon binding, experiments were also performed in 10 mM Tris, pH 8.0 at 25°C. The values of ΔH measured in Tris buffer (enthalpy of ionization, 11.51 kcal mol^{-1} at 25°C) did not differ significantly from those measured in

phosphate buffer (enthalpy of ionization, 1.22 kcal mol^{-1} at 25°C (24)) showing that the contribution of buffer titration to the observed ΔH is negligible. As shown in Table 1, ΔH also does not vary significantly upon addition of 100 mM NaCl, or upon changing the pH from 8.0 to 7.0.

The enthalpy of HH10/HEL association declines linearly from −17.4 kcal mol^{-1} at 10°C to −24.1 kcal mol^{-1} at 37°C, giving a constant value of ΔCp of −248.1 ± 1.0 cal mol^{-1} K^{-1} (Table 2). The SPR-derived ΔG values for each temperature (Table 2) and the experimentally determined values of ΔH as a function of temperature were used to calculate ΔS values as a function of temperature. HH10/HEL association is accompanied by a favorable enthalpy change and unfavorable entropy change at all temperatures studied.

The energetics of titration of HH10, as well as HH8 and HH26, with JQL are presented in Table 3. Buffer controls for proton liberation or uptake as described above indicated that no significant proton liberation/uptake occurs upon JQL/HH10 association.

The SPR-derived ΔG values and the ITC- determined values of ΔH as a function of temperature were used to calculate values of ΔS over the temperature range of interest (Table 3). The enthalpy of HH10/JQL association declines linearly from −5.8 kcal mol^{-1} at 10.0°C to −14.2 kcal mol^{-1} at 37.0°C, yielding a constant ΔC_p of −310.7 ± 8.5 cal mol^{-1} K^{-1}.

Association energetics of HH8 and HH26 with HEL and JQL

These systems were studied by the same methods as described above for HH10, though in less detail (Table 2). Stoichiometric equivalence ratios were as close or closer to unity as observed for HH10, and experimental errors were similar to those for the HH10 system (average standard error 2.5%). The affinity of HH26 for JQL was low enough to be determined calorimetrically (Figure 2); all ΔG values used to calculate the derived thermodynamic parameters in Table 2–Table 4 were SPR-derived/estimated. It is noteworthy that the calorimetrically-determined affinity for HH26/JQL association at 25 °C is 1.32×10^{-7} M, giving a total change in free energy upon binding ΔG = −9.58 kcal mol^{-1} which compares well with the value of −8.5 kcal mol^{-1} obtained using the very different method of SPR.

Discussion

Antibody association with HEL

Association of all three antibodies with HEL is enthalpically driven with an entropic penalty at all temperatures from 10 to 37°C with the sole exception of H8 at 10°C with a small favorable entropy. ΔH declines linearly with temperature, i.e. it becomes more favorable at higher temperatures. The values of ΔC_p observed are comparable to those obtained in previous studies of protein-protein associations. Calculated values of $T\Delta S$ become much less favorable as temperature increases, changing on average by 7.6 kcal mol^{-1} over the temperature range studied, while the values of experimental and estimated SPR-derived ΔG on average change by less than 1 kcal mol^{-1} over this range of temperatures; thus, a nearly complete enthalpy-entropy compensation occurs in this system. In all three complexes, unfavorable changes in enthalpy are compensated by reductions in unfavorable entropy as temperature decreases, typical of other antibody-antigen interactions (25–27).

We have shown elsewhere that the association kinetics of these complexes are best described by a two-step model corresponding to rapid formation of an intermediate/encounter complex, followed by a slower annealing or docking to a more stable complex (9–11,23). We have also demonstrated that the first step of the HEL association is usually entropically driven, while the docking step is enthalpically driven with a large entropic penalty (C.A. Lipschultz *et al*., unpublished data).

Association of the more-specific HH26-HEL complex is characterized by a higher favorable enthalpy change than HH8-HEL at all temperatures studied here, with the difference becoming more apparent at lower temperatures. The HH26-HEL interface has more hydrogen bonds, both inter-and intra-molecular, and stronger electrostatic interactions than the other two complexes (6,28). Among the HEL complexes, at each temperature studied the HH8-HEL complex has the lowest enthalpy of association, consistent with this complex having the smallest number of stabilizing hydrogen bonds and electrostatic interactions.

The entropy changes of association of the three antibodies with HEL are generally negative (unfavorable). Of the three antibody complexes with HEL, that of HH8 shows the smallest unfavorable ΔS at every temperature (Table 2). The HH8-HEL entropic change is in fact positive (favorable) at 10°C. The change in specific heat capacity, which in part reflects the extent of burial of hydrophobic interfacial residues upon association, is larger for the HH8-HEL complex (-363.9 cal mol^{-1} K^{-1}) than for HH26-HEL complex (-238.8 cal mol^{-1} K^{-1}). This is consistent with the results of structural and computational studies showing that the binding site of HH8 involves more hydrophobic residues compared to the other two antibodies (6,28–30).

It is unusual for the interaction of an antibody with a large protein antigen to have a favorable (positive) entropy change, although associations of smaller proteins with (relatively hydrophobic) drug molecules are frequently entropically driven (31). Favorable entropy changes of association could arise in part from the contributions of the mobility of water molecules and backbone and side chain atoms in the interface, implying a lack of “tight fit” or alternatively, an association accompanied by water exclusion and an interaction dominated by hydrophobic interactions. A fully affinity-matured antibody would be expected to show close shape complementary to its antigen, and a lack of fit would indicate either that the antibody is incompletely matured, or that it has a certain degree of intrinsic cross-reactivity. A structural comparison revealed that the combining site of the chimeric HH H8L10 (heavy chain of HH8 refolded with the light chain of HH10) showed higher surface complementarity to HEL than either HH26 or HH10 (6). HH8, which is a high-affinity (higher than HH10 or HH26) antibody obtained from the hyperimmune (memory) response (7,32), belongs to the latter category. Structural studies have shown that during affinity maturation, somatic mutation increases the number of hydrophobic residues in the combining site at the expense of polar residues (6). In addition, detailed analyses of site-directed mutants of the anti-HEL antibody D1.3 supported the hypothesis that the entropic changes in the complex were most likely related to hydrophobic interactions (33).

Antibody association with JQL

The HH26-JQL complex was the only complex with affinity low enough to be reliably measured by ITC (Figure 2), the association constant calculated from ITC data agrees with that obtained by measuring the kinetics by SPR techniques. Compared to association with HEL, association of all three antibodies with JQL involves much smaller enthalpic contributions, compensated by corresponding larger favorable entropy changes. Entropic changes of association for all three complexes at 25°C and 10°C are positive. Among the three antibodies, the HH26-JQL complex has both the smallest favorable enthalpy and the largest favorable entropy of association at 37 and 25°C, respectively. Despite this compensation, the affinity of HH26 for JQL is about 39 times lower than its affinity for HEL. HH8 shows less specificity, with an affinity for JQL only about 7 times lower than that for HEL (5). As in the antibody-HEL complexes, ΔC_p of the HH8-JQL complex is the largest among the three JQL complexes while that of the HH26-JQL complex is the smallest, suggesting that in the HH8-JQL complex more hydrophobic residues are involved in mediating the interaction. An overlay of the x-ray crystallographic structure of JQL (34), PDB code: 2IHL with HEL (in the HH10-HEL complex)

reveals that the conformation of the backbone of JQL around positions 101, 102 and 103 differs substantially from that of uncomplexed HEL. The C^{α} atoms of JQL, at positions 102 and 103, are shifted by 5.6 and 4.1 Å respectively, relative to their corresponding positions in HEL (29). JQL has the residues Val and His at positions 102 and 103 instead of the Gly and Asn respectively present in HEL. In order to accommodate the structural differences of JQL (e.g. to avoid steric clashes) the paratope of any of the antibodies would necessarily undergo some conformational changes compared to their conformations in the structures with HEL (28). Molecular modeling studies suggest that more-extensive intramolecular salt and hydrogen bond networks would render HH10 and HH26 less likely to undergo such rearrangements than HH8 (28,29).

The amino acid sequence of JQL differs from HEL in six positions, the most notable epitope change being the R21Q mutation. HEL residue Arg21 is an epitope “hot spot”, and is among the largest contributors of free energy to these complexes (9,13,35,36). HH10 makes three hydrogen bonds with this residue and several non-bonded contacts (8,29,35–38). Mutating this arginine to glutamine, as in JQL, would lead to the loss of at least two hydrogen bonds and several non-bonded contacts. The loss of these contacts would result in a corresponding decrease in the favorable enthalpic driving force.

Enthalpic contributions dominate antibody specificity

Previous SPR-based studies have demonstrated that epitope mutations affect the kinetics of cross-reactive and specific antibodies to varying degrees; however, the thermodynamic mechanisms that actually mediate cross-reactive or specific behavior are not understood. To investigate this issue, the mutational differences of the energetic components, ($\Delta\Delta H_{JQL\text{-}HEL}$, ($\Delta\text{-}T\Delta S)_{JQL\text{-}HEL}$ and $\Delta\Delta G_{JQL\text{-}HEL}$) were calculated for the three antibodies (Table 4). The association of the highly-specific HH26 with JQL compared to HEL involves both a large loss of favorable enthalpy change and a gain in favorable entropy change. The values of the corresponding changes for the association of HH8 are the smallest, and those for HH10 are intermediate.

In protein-protein associations, enthalpic change largely represents the structural composition of hydrogen bonds, electrostatic interactions and water-mediated interactions (31). The specificity of an antibody is the selective recognition of its ligand through specific interactions between a select set of residues in the interacting surfaces, and hydrogen bonds and electrostatic interactions are the predominant mediators of this specificity (31,39,40). While HH10 has the largest net change in enthalpy in its association with both HEL and JQL, the mutational loss of association enthalpy, $\Delta\Delta H_{JQL\text{-}HEL}$ is generally the largest for HH26 at 37°C, and those for both HH10 and HH26 are greater than for HH8 at all temperatures (Table 4; note the similar values for HH26 and HH10 at 25°C and 10°C; also note that the values for HH26 are within the standard error of the values for HH10 at both temperatures, Table S1). Though these losses of enthalpic driving force are partly compensated by more-favorable entropy changes of association in both antibodies, there is a net reduction in affinity of HH26 for JQL of approximately 39-fold. This probably reflects the loss of some important stabilizing interactions found in both complexes and suggests that the *specificity* of the antibodies is mediated by interactions that are predominantly *enthalpic in nature*. Structure-based comparison of the numbers of geometry-sensitive hydrogen bonds, salt links and electrostatic interactions with antigen shows that among the three complexes, that of HH26 has the largest number of each (6,28,29), and that the contribution of intermolecular electrostatic forces is greatest in the HH26 complex (6,12,28,29). In the modeled complexes of the three antibodies with HEL, HH26 forms 18 hydrogen bonds with HEL in comparison to the 11 hydrogen bonds formed by HH8, which correlates well with the current observation that the smallest change in enthalpic contribution is associated with HH8. The complexes of HH10 and HH26 derive

stability mainly from enthalpic energy while the smaller mutational loss of association enthalpy for HH8 (the smallest of the three) implies that this antibody is able to maintain most of the (predominantly hydrophobic) interactions (6) crucial for its recognition, even with mutant antigen. The magnitude of loss of enthalpic driving force for HH10 with JQL correlates with its degree of specificity, which is intermediate. These conclusions agree with those of Kumagai *et al.* (41,42).

Configurational entropy mediates antibody cross-reactivity

The total change in entropy ΔS is the summation of solvent, configurational and cratic effects, represented by ΔS_{solv}, ΔS_{conf} and ΔS_{crat}, respectively (43). Upon formation of the antibody-antigen complex, the variation of arrangement of water molecules around polar and apolar patches is reflected in ΔS_{solv}, while the changes in configurational freedom of backbone and side chains of both antibody and antigen is given by ΔS_{conf}. ΔS_{crat} represents the loss of translational and rotational degrees of freedom for the associating proteins and is empirically determined to be −8 cal K^{-1} mol^{-1}. ΔS_{solv} is given by $\Delta C_p \ln(T/T_s^*)$, where T_s^* is taken as 112 °C, the temperature at which the aqueous dissolution of apolar compounds is independent of the apolar surface area. The values of ΔS_{solv} and ΔS_{conf} thus calculated are listed in Table 2 and Table 3 for antibody associations with HEL and JQL, respectively.

At all temperatures studied, the complexes of less-specific HH8 with HEL and JQL have the largest favorable solvent contribution to entropy, as well as the largest unfavorable configurational entropic penalty to total entropic change with the sole exception of HH10-JQL at 10°C. On the other hand, the complexes of the highly-specific HH26 exhibit the smallest favorable ΔS_{solv} as well as the smallest unfavorable ΔS_{conf} at all temperatures, while the corresponding changes for HH10 lie in between (note the similar ΔS_{conf} for HEL complexes of HH10 and HH26). Since these three related antibodies are known to recognize the same structurally-characterized epitope on both HEL and JQL, the differences observed in configurational entropy are probably primarily due to the structural differences among the antibody binding sites. Previous computational studies showed that the binding site of HH26 is likely to be the most rigid, because it is stabilized by the largest number of intramolecular salt-bridges (28,29). In contrast, the binding site of HH8 lacks these stabilizing interactions, making it the most flexible and allowing it to adopt alternate conformations (28,29,44). The binding site of HH10 has a moderate number of intramolecular salt-bridges and was predicted to be of intermediate flexibility (28,29,44). The largest changes of configurational entropy (Table 2 & Table 3) were seen for flexible HH8, consistent with the idea that its binding site undergoes the largest conformational rearrangement upon association. The complexes of HH8 are thus very likely formed by molecular processes most typical of induced fit associations. The conformational rearrangements in the complexes of HH8 also result in the largest buried surface area and the greatest degree of intermolecular surface complementarity (28,29,44). The increased complementarity is not necessarily due to structural rearrangements only in those segments with sequence changes in complementarity determining regions (CDR) unique to HH8, but also likely involves subtle structural rearrangements in the other CDR's as well as in HEL. This would lead to increased complementarity both of the entire binding interface and in the areas of the interface buried upon complex formation (41). The intrinsic ability of HH8 to reorganize its binding site when it encounters a mutant antigen correlates with its cross-reactivity. Conformational rearrangement may also allow preservation of hydrogen bonds and electrostatic interactions that would otherwise be lost, leading to the observed smallest $\Delta\Delta H$ of antigen mutation (Table 4).

In contrast, the configurational entropic effects of HH26 complexes may reflect the lower degree of conformational rearrangement exhibited by this antibody. Structural studies comparing movements of CDR2 of the heavy chain support this hypothesis (6). Although this

antibody has the largest overall favorable mutational $\Delta(-T\Delta S)$, this falls short of compensating for the losses of favorable ΔH. The loss of tight binding in HH26-JQL complex, evidenced by the gain in configurational freedom, is also supported by the further reduction in the already-smallest estimated buried surface area. If the binding site of HH26 is unable to adopt alternate conformations that could lead to new interactions, the result would be increased configurational freedom that does not compensate for the loss of bond energy. The inability of its binding site to adopt alternate conformations, which agrees with modeling predictions and structural studies (6,29), is a possible cause of its relative intolerance of epitope mutations. As the binding site of HH26 undergoes minimal structural perturbation, the association of this antibody with its antigen can be best described as a “lock and key” process.

The apparent conformational flexibility of HH8, on the other hand, helps this antibody to form new interactions by conformational rearrangement of its binding site when it encounters a mutant antigen. The higher affinity of HH8 for both HEL and variant antigens likely involves both an increase in favorable enthalpy change of association due to localized interface interactions, as well as compensatory decreases in favorable enthalpy and unfavorable entropy due to other mutations which allow the flexibility (41). In addition, at any given temperature the HH8 complexes with both antigens have the highest favorable solvent portion of the entropy term compared to the respective complexes of either HH10 or HH26. This is consistent with the conclusion of Mariuzza and colleagues that hydrophobic interactions are a primary contributor to complex stability (6,33,37). The changes observed in the corresponding energetic parameters of HH10 are moderate, indicating that it is able to partially compensate for some of the lost interactions when it encounters a variant antigen by undergoing conformational rearrangement, albeit to a lesser extent than HH8.

In conclusion, here we demonstrate that the energetic bases of specific and cross-reactive association are fundamentally different. Specificity is often manifested in a pre-organized combining site that mediates conserved interactions within the complex, as exhibited by HH26. While HH26 incurs only a small configurational entropic penalty in associating with the mutant antigen JQL, the inability of its rigidly pre-configured binding site to accommodate the mutant antigen precludes the formation of new interactions that could otherwise moderate its large loss of enthalpic driving force. Cross-reactivity, on the other hand, is generally associated with a more “generic,” flexible binding site and less conserved interactions as evident in the association of HH8 with the mutant antigen. The binding site of HH8 probably adopts alternate conformations at the cost of large entropic penalties, but forms intermolecular interactions (specific or non-specific) that would be otherwise lost with mutant antigen.

Supplementary Material

Refer to Web version on PubMed Central for supplementary material.

Acknowledgments

This research was supported by Welch Foundation (E-1264), the Alliance for Nanohealth, NIH, and in part by the Intramural Research Program of NIH, National Cancer Institute, Center for Cancer Research.

References

1. Lo Conte L, Chothia C, Janin J. The atomic structure of protein-protein recognition sites. J. Mol. Biol 1999;285:2177–2198. [PubMed: 9925793]
2. Mariuzza RA, Poljak RJ, Schwarz FP. The energetics of antigen-antibody binding. Res. Immunol 1994;145:70–72. [PubMed: 8008972]
3. Sundberg EJ, Mariuzza RA. Molecular recognition in antibody-antigen complexes. Adv. Protein Chem 2002;61:119–160. [PubMed: 12461823]

4. Lavoie TB, Drohan WN, Smith-Gill SJ. Experimental analysis by site-directed mutagenesis of somatic mutation effects on affinity and fine specificity in antibodies specific for lysozyme. J. Immunol 1992;148:503–513. [PubMed: 1729369]
5. Lavoie TB, Mohan S, Lipschultz CA, Grivel JC, Li Y, Mainhart CR, Kam-Morgan LN, Drohan WN, Smith-Gill SJ. Structural differences among monoclonal antibodies with distinct fine specificities and kinetic properties. Mol. Immunol 1999;36:1189–1205. [PubMed: 10698321]
6. Li Y, Li H, Yang F, Smith-Gill SJ, Mariuzza RA. X-ray snapshots of the maturation of an antibody response to a protein antigen. Nat. Struct. Biol 2003;10:482–488. [PubMed: 12740607]
7. Newman MA, Mainhart CR, Mallett CP, Lavoie TB, Smith-Gill SJ. Patterns of antibody specificity during the BALB/c immune response to hen eggwhite lysozyme. J. Immunol 1992;149:3260–3272. [PubMed: 1431104]
8. Padlan EA, Silverton EW, Sheriff S, Cohen GH, Smith-Gill SJ, Davies DR. Structure of an antibody-antigen complex: crystal structure of the HyHEL-10 Fab-lysozyme complex. Proc. Natl. Acad. Sci. U. S. A 1989;86:5938–5942. [PubMed: 2762305]
9. Li Y, Lipschultz CA, Mohan S, Smith-Gill SJ. Mutations of an epitope hot-spot residue alter rate limiting steps of antigen-antibody protein-protein associations. Biochemistry 2001;40:2011–2022. [PubMed: 11329268]
10. Lipschultz CA, Li Y, Smith-Gill S. Experimental design for analysis of complex kinetics using surface plasmon resonance. Methods 2000;20:310–318. [PubMed: 10694453]
11. Lipschultz CA, Yee A, Mohan S, Li Y, Smith-Gill SJ. Temperature differentially affects encounter and docking thermodynamics of antibody--antigen association. J. Mol. Recognit 2002;15:44–52. [PubMed: 11870921]
12. Sinha N, Smith-Gill SJ. Electrostatics in protein binding and function. Curr Protein Pept Sci 2002;3:601–614. [PubMed: 12470214]
13. Smith-Gill SJ, Lavoie TB, Mainhart CR. Antigenic regions defined by monoclonal antibodies correspond to structural domains of avian lysozyme. J. Immunol 1984;133:384–393. [PubMed: 6202787]
14. Smith-Gill, SJas; E.E.. The Immune Response to Structurally Defined Proteins: The Lysozyme Model. New York: Adenine press; 1989.
15. Hibbits KA, Gill DS, Willson RC. Isothermal titration calorimetric study of the association of hen egg lysozyme and the anti-lysozyme antibody HyHEL-5. Biochemistry 1994;33:3584–3590. [PubMed: 8142356]
16. Shugar D. The measurement of lysozyme activity and the ultra-violet inactivation of lysozyme. Biochim. Biophys. Acta 1952;8:302–309. [PubMed: 14934741]
17. Aune KC, Tanford C. Thermodynamics of the denaturation of lysozyme by guanidine hydrochloride. I. Dependence on pH at 25 degrees. Biochemistry 1969;8:4579–4585. [PubMed: 5389440]
18. Jolles P. Lysozymes: a chapter of molecular biology. Angew. Chem. Int. Ed. Engl 1969;8:227–239. [PubMed: 4977569]
19. Gill SC, von Hippel PH. Calculation of protein extinction coefficients from amino acid sequence data. Anal. Biochem 1989;182:319–326. [PubMed: 2610349]
20. Kabat, EA.; W; T.T.; perry, HM.; Gottesman, KS.; Foeller, C. Sequences of Proteins of Immunoligical Interest. Vol. 5th ed.. Bethesda, MA: Diane Books Publishing Co, National Institutes of Health; 1991.
21. Xavier KA, Willson RC. Association and dissociation kinetics of anti-hen egg lysozyme monoclonal antibodies HyHEL-5 and HyHEL-10. Biophys. J 1998;74:2036–2045. [PubMed: 9545062]
22. Wiseman T, Williston S, Brandts JF, Lin LN. Rapid measurement of binding constants and heats of binding using a new titration calorimeter. Anal. Biochem 1989;179:131–137. [PubMed: 2757186]
23. Kourentzi K, Srinivasan M, Smith-Gill SJ, Willson RC. Conformational flexibility and kinetic complexity in antibody-antigen interactions. J. Mol. Recognit 2008;21:114–121. [PubMed: 18383102]
24. Morin PE, Freire E. Direct calorimetric analysis of the enzymatic activity of yeast cytochrome c oxidase. Biochemistry (Mosc) 1991;30:8494–8500.
25. Goldbaum FA, Schwarz FP, Eisenstein E, Cauerhff A, Mariuzza RA, Poljak RJ. The effect of water activity on the association constant and the enthalpy of reaction between lysozyme and the specific antibodies D1.3 and D44.1. J. Mol. Recognit 1996;9:6–12. [PubMed: 8723314]

26. Yokota A, Tsumoto K, Shiroishi M, Kondo H, Kumagai I. The role of hydrogen bonding via interfacial water molecules in antigen-antibody complexation. The HyHEL-10-HEL interaction. J. Biol. Chem 2003;278:5410–5418. [PubMed: 12444085]
27. Ysern X, Fields BA, Bhat TN, Goldbaum FA, Dall'Acqua W, Schwarz FP, Poljak RJ, Mariuzza RA. Solvent rearrangement in an antigen-antibody interface introduced by site-directed mutagenesis of the antibody combining site. J. Mol. Biol 1994;238:496–500. [PubMed: 8176740]
28. Sinha N, Mohan S, Lipschultz CA, Smith-Gill SJ. Differences in electrostatic properties at antibody-antigen binding sites: implications for specificity and cross-reactivity. Biophys. J 2002;83:2946–2968. [PubMed: 12496069]
29. Mohan S, Sinha N, Smith-Gill SJ. Modeling the binding sites of anti-hen egg white lysozyme antibodies HyHEL-8 and HyHEL-26: an insight into the molecular basis of antibody cross-reactivity and specificity. Biophys. J 2003;85:3221–3236. [PubMed: 14581222]
30. Smith-Gill SJ, Mainhart C, Lavoie TB, Feldmann RJ, Drohan W, Brooks BR. A three-dimensional model of an anti-lysozyme antibody. J. Mol. Biol 1987;194:713–724. [PubMed: 3656404]
31. Todd MJ, Freire E. The effect of inhibitor binding on the structural stability and cooperativity of the HIV-1 protease. Proteins 1999;36:147–156. [PubMed: 10398363]
32. Smith-Gill SJ, Mainhart CR, Lavoie TB, Rudikoff S, Potter M. VLVH expression by monoclonal antibodies recognizing avian lysozyme. J. Immunol 1984;132:963–967. [PubMed: 6418816]
33. Sundberg EJ, Urrutia M, Braden BC, Isern J, Tsuchiya D, Fields BA, Malchiodi EL, Tormo J, Schwarz FP, Mariuzza RA. Estimation of the hydrophobic effect in an antigen-antibody protein-protein interface. Biochemistry 2000;39:15375–15387. [PubMed: 11112523]
34. Chitarra V, Alzari PM, Bentley GA, Bhat TN, Eisele JL, Houdusse A, Lescar J, Souchon H, Poljak RJ. Three-dimensional structure of a heteroclitic antigen-antibody cross-reaction complex. Proc. Natl. Acad. Sci. U. S. A 1993;90:7711–7715. [PubMed: 8356074]
35. Kam-Morgan LN, Smith-Gill SJ, Taylor MG, Zhang L, Wilson AC, Kirsch JF. High-resolution mapping of the HyHEL-10 epitope of chicken lysozyme by site-directed mutagenesis. Proc. Natl. Acad. Sci. U. S. A 1993;90:3958–3962. [PubMed: 7683415]
36. Pons J, Rajpal A, Kirsch JF. Energetic analysis of an antigen/antibody interface: alanine scanning mutagenesis and double mutant cycles on the HyHEL-10/lysozyme interaction. Protein Sci 1999;8:958–968. [PubMed: 10338006]
37. Rajpal A, Taylor MG, Kirsch JF. Quantitative evaluation of the chicken lysozyme epitope in the HyHEL-10 Fab complex: free energies and kinetics. Protein Sci 1998;7:1868–1874. [PubMed: 9761468]
38. Taylor MG, Rajpal A, Kirsch JF. Kinetic epitope mapping of the chicken lysozyme.HyHEL-10 Fab complex: delineation of docking trajectories. Protein Sci 1998;7:1857–1867. [PubMed: 9761467]
39. Kwong PD, Doyle ML, Casper DJ, Cicala C, Leavitt SA, Majeed S, Steenbeke TD, Venturi M, Chaiken I, Fung M, Katinger H, Parren PW, Robinson J, Van Ryk D, Wang L, Burton DR, Freire E, Wyatt R, Sodroski J, Hendrickson WA, Arthos J. HIV-1 evades antibody-mediated neutralization through conformational masking of receptor-binding sites. Nature 2002;420:678–682. [PubMed: 12478295]
40. Myszka DG, Sweet RW, Hensley P, Brigham-Burke M, Kwong PD, Hendrickson WA, Wyatt R, Sodroski J, Doyle ML. Energetics of the HIV gp120-CD4 binding reaction. Proc. Natl. Acad. Sci. U. S. A 2000;97:9026–9031. [PubMed: 10922058]
41. Kumagai I, Nishimiya Y, Kondo H, Tsumoto K. Structural consequences of target epitope-directed functional alteration of an antibody. The case of anti-hen lysozyme antibody, HyHEL-10. J. Biol. Chem 2003;278:24929–24936. [PubMed: 12709438]
42. Nishimiya Y, Tsumoto K, Shiroishi M, Yutani K, Kumagai I. Thermodynamic consequences of grafting enhanced affinity toward the mutated antigen onto an antibody. The case of anti-lysozyme antibody, HyHEL-10. J. Biol. Chem 2000;275:12813–12820. [PubMed: 10777579]
43. Murphy KP, Freire E, Paterson Y. Configurational effects in antibody-antigen interactions studied by microcalorimetry. Proteins 1995;21:83–90. [PubMed: 7539913]
44. Sinha N, Smith-Gill SJ. Molecular dynamics simulation of a high-affinity antibody-protein complex: the binding site is a mosaic of locally flexible and preorganized rigid regions. Cell Biochem. Biophys 2005;43:253–273. [PubMed: 16049350]

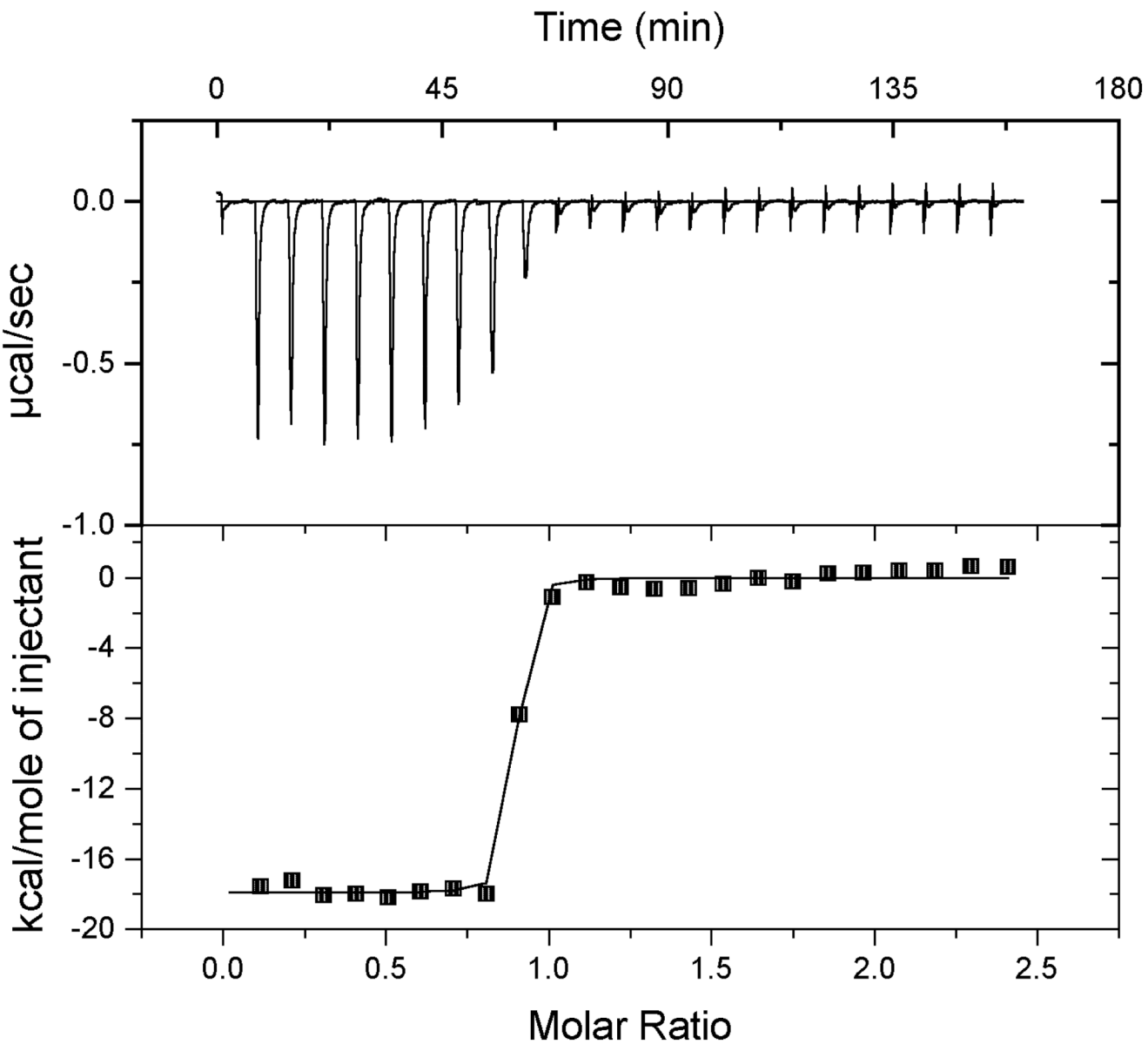

Figure 1.
Calorimetric titration profile of association of HH8 with HEL at 25°C.

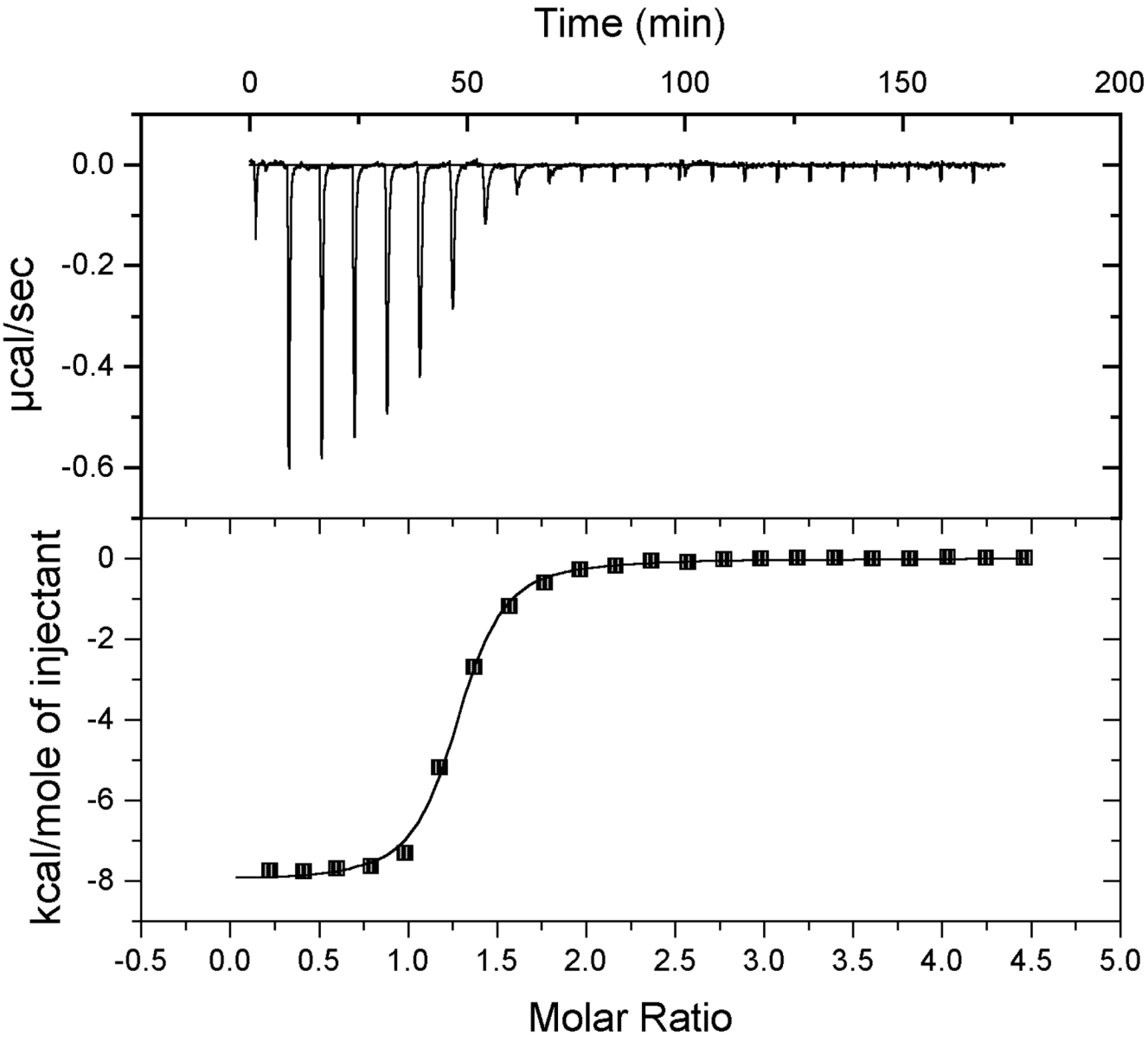

Figure 2.
Calorimetric titration profile of association of HH26 with JQL at 25°C.

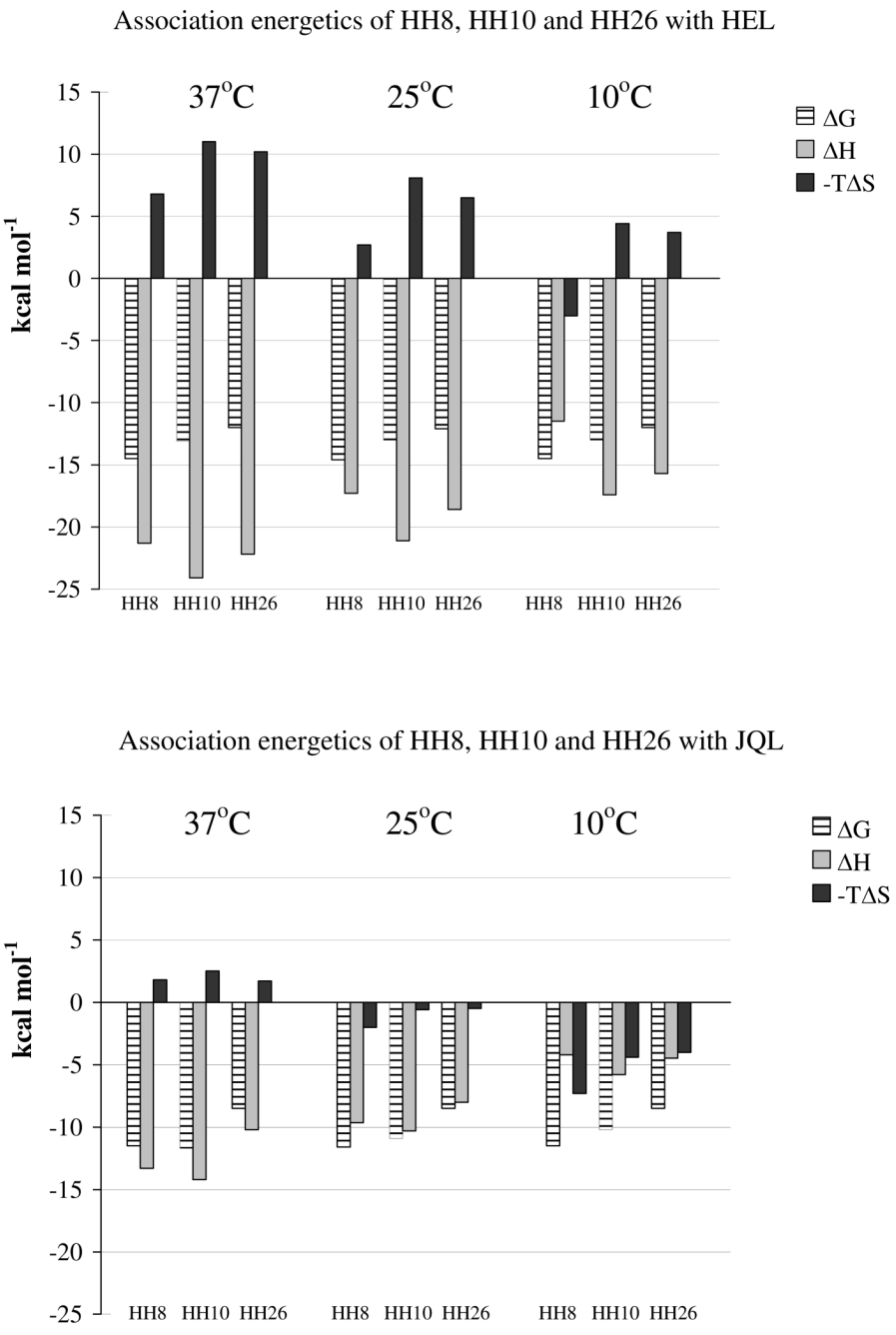

Figure 3.
Energetics of association of HH8, HH10 and HH26 with HEL (Top) and JQL (Bottom).

Table 1

Titration calorimetry results for HH10 with hen egg lysozyme (HEL) and Japanese quail egg lysozyme (JQL).

Buffer	Lysozyme	Temperature °C	ΔH kcal mol^{-1}	Equivalence Ratio
10 mM Na PO_4, pH 8.0	HEL	37.0	−24.1±0.28	0.75±0.05
10 mM Na PO_4, pH 8.0	JQL	37.0	−14.2±0.20	0.92±0.07
10 mM Na PO_4, pH 8.0	HEL	25.0	−21.1±0.83	0.70±0.04
10 mM Na PO_4, pH 8.0	JQL	25.0	−10.3±0.37	0.78±0.12
10 mM Na PO_4, pH 8.0	HEL	10.0	−17.4±0.76	0.86±0.02
10 mM Na PO_4, pH 8.0	JQL	10.0[a]	−5.8±0.23	0.72±0.08
10 mM Tris, pH 8.0	HEL	25.0	−20.5±0.21	0.78±0.01
10 mM Tris, pH 8.0	JQL	25.0	−9.8±0.17	0.78±0.28
10 mM Na PO_4, pH 8.0 + 100 mM NaCl	HEL	25.0	−19.7±0.56	0.92±0.01
10 mM Na PO_4, pH 7.0	HEL	25.0	−20.6±0.28	0.72±0.06

[a] Actual experimental temperature 13.5°C; ΔH value at 10°C extrapolated using ΔCp. All other experimental temperatures were within 0.3° of reported temperature.

Table 2

Energetics of association of HEL with HH8, HH10 and HH26

mAb	T °C	ΔG^a kcal mol^{-1}	ΔH kcal mol^{-1}	ΔC_p cal mol^{-1} K^{-1}	ΔS cal mol^{-1} K^{-1}	$-T\Delta S$ kcal mol^{-1}	$\Delta S_{solv}{}^b$ cal mol^{-1} K^{-1}	$\Delta S_{conf}{}^b$ cal mol^{-1} K^{-1}
HH8	37	−14.5	−21.3		−21.6	6.8	78.8	−92.7
	25	−14.6 ±0.1	−17.3±0.4	−363.9±15.1	−9.1±1.49	2.7±0.4	93.2±3.9	−94.3±4.1
	10	−14.5	−11.5		10.5	−3.0	112.0	−93.5
HH10	37	−13.1±0.2	−24.1±0.3		−35.5±1.2	11.0±0.4	53.8±0.2	−81.2±1.2
	25	−13.0±0.1	−21.1±0.8	−248.1±1.0	−27.2±2.7	8.1±0.8	63.6±0.3	−82.7±2.7
	10	−13.0±0.1	−17.4±0.8		−15.5±2.9	4.4±0.8	76.4±0.3	−83.9±2.9
HH26	37	−12.0	−22.2		−32.9	10.2	51.7	−76.6
	25	−12.3±0.1	−18.6±4.7	−238.8±30.3	−21.1±1.6	6.3±0.5	61.2±7.8	−75.0±7.9
	10	−12.0	−15.7		−13.1	3.7	73.5	−78.9

[a] Experimental values (± 1 SD) at all 3 temperatures for HH10; for HH8 and HH26 experimental values (± 1 SD) at 25°C and estimated values at 10 and 37°C using the non-linear van't Hoff equation as described in Materials & Methods.

[b] $\Delta S = \Delta S_{solv} + \Delta S_{conf} + \Delta S_{crat}$; $\Delta S_{solv} = \Delta C_p{}^* \ln(T/T_s{}^*)$, $T_s{}^* = 385°K$; $\Delta S_{crat} = -8$ cal K^{-1} mol^{-1}(43)

Table 3

Energetics of association of JQL with HH8, HH10 and HH26.

mAb	T °C	ΔG^a kcal mol^{-1}	ΔH kcal mol^{-1}	ΔC_p cal mol^{-1} K^{-1}	ΔS cal mol^{-1} K^{-1}	$-T\Delta S$ kcal mol^{-1}	ΔS_{solv} [b] cal mol^{-1} K^{-1}	ΔS_{conf} [b] cal mol^{-1} K^{-1}
HH8	37	−11.4	−13.3		−6.1	1.9	73.3	−70.9
	25	−11.5±0.3	−9.6±0.2	−338.1±16.4	6.2±1.3	−1.9±0.4	86.6±4.2	−72.0±44
	10	−11.5	−4.2		25.8	−7.2	104.1	−70.3
HH10	37	−11.7±1.0	−14.2±0.2		−8.1±3.3	2.5±1.0	67.3±1.9	−67.4±3.8
	25	−10.9±1.2	−10.3±0.4	−310.7±8.5	2.3±3.3	−0.7±1.3	79.6±2.2	−69.6±4.8
	10	−10.2±0.7	−5.8±0.2		15.5±2.6	−4.4±0.7	95.6±2.6	−72.1±3.7
HH26	37	−8.5	−10.2		−5.5	1.7	46.2	−43.7
	25	−8.5±0.7	−8.0±0.2	−213.2±15.6	1.7±2.4	−0.5±0.7	54.6±4.0	−44.9±4.7
	10	−8.5	−4.5		14.0	−3.9	65.6	−43.4

[a] Experimental values (± 1 SD) at all 3 temperatures for HH10; for HH8 and HH26 experimental values (± 1 SD) at 25°C and estimated values at 10 and 37°C using the non-linear van't Hoff equation as described in Materials & Methods.

[b] $\Delta S = \Delta S_{solv} + \Delta S_{conf} + \Delta S_{crat}$; $\Delta S_{solv} = \Delta C_p{}^* \ln(T/T_s{}^*)$, $T_s = 385^\circ$K; $\Delta S_{crat} = -8$ cal K^{-1}mol^{-1}(43)

Table 4

Effect of JQL mutations on the association energy changes of HH8, HH10 and HH26 complexes.

mAb	T °C	$\Delta\Delta G_{(JQL-HEL)}$ kcal mol^{-1}	$\Delta\Delta H_{(JQL-HEL)}$ kcal mol^{-1}	$\Delta(-T\Delta S)_{(JQL-HEL)}$ kcal mol^{-1}	$\Delta\Delta S_{solv}$ cal mol^{-1} K^{-1}	ΔS_{conf} cal mol^{-1} K^{-1}
HH8	37	3.0	8.0	−5.0	−5.6	21.8
	25	3.0±0.3	7.7±0.5	−4.7±0.6	−6.6±5.7	22.3±6.0
	10	3.0	7.3	−4.3	−7.9	23.2
HH10	37	1.4±1.0	9.9±0.4	−8.5±1.1	13.6±1.9	13.9±4.0
	25	2.1±1.2	10.8±0.9	−8.7±1.5	16.0±2.2	13.2±5.5
	10	2.8±0.7	11.6±0.8	−8.8±1.1	19.3±2.6	11.8±4.7
HH26	37	3.5	12.0	−8.5	−5.5	32.8
	25	3.6±0.7	10.6±0.5	−7.0±0.9	−6.6±8.7	30.1±9.2
	10	3.5	11.2	−7.7	−7.9	35.2